KINEMATIC TRAJECTORIES RECONSTRUCTION BASED ON MOTORS ENCODERS FEEDBACK FOR A ROVER SKID-STEERING ROBOT

Nicola Ivan Giannoccaro*

Dipartimento di Ingegneria dell'Innovazione, Università del Salento

via per Monteroni 73100 Lecce, Italy

*email: ivan.giannoccaro@unisalento.it; Tel. +390832297813

Submitted:Sep. 15, 2015 ***Accepted:Nov. 10, 2015*** ***Published:Dec. 1, 2015***

Abstract- In this paper some procedures for accurately defining the kinematic trajectories described by skid-steering robots by using only the kinematic data of the wheels (or tracks) are presented and discussed. These procedures have been analysed with several experimental tests carried out moving a rover skid-steering robot on different surfaces. The particularity of the skid steering mobile robots is the presence of the high slippage effects that heavily influence the correct kinematic reconstruction by using the classical kinematic equation. For this reason, the possibility of using particular strategies based on the instantaneous centre radiuses is here considered; these strategies use parameters such as the equivalent 'carriageway', the slipping coefficients and the slipping ratio for including the effect of vehicle dynamics. Moreover, the effect of different surfaces is evident on the parameters that characterize the considered strategies for kinematic reconstruction; anyway, the high repeatability of the experiments carried out on the same conditions and a certain trend of the slipping ratio that seems to characterise the different types of surfaces, allow foreseeing positive developments of the considered strategies. The experiments have been carried out on a particular skid-steering robot (rover 4WD1); the generalization of the results for other types of skid-steering robot may be easily foreshadowed.
The original value of the paper is related to the systematic experimental validation of the procedures indicated and to the comments that may be very useful in defining the limits of the procedure for the kinematic reconstruction with high slipping effects.

Index terms*:* Kinematic analysis, Skid-steering robots, Position measurements.

I. INTRODUCTION

The skid-steering robots are becoming very popular for their simplicity due to the lack of a steering mechanism as large industrial and agricultural vehicles. Their characteristic lies in the possibility of changes vehicle direction by adjusting the speed of the left and right side wheels or tracks. The simplicity, robustness, and zero-radius turn capability of skid-steering make it an excellent choice for all-terrain and tele-operated vehicles, but the disadvantage of these robots is the difficult to apply the classical kinematic equation, for the high slippage that occurs during the manoeuvres. Hence, it is quite difficult to predict the future position of a skid-steer robot with a certain accuracy. Moreover, the kinematic behaviour of the robot is strongly influenced by the physical properties of the terrain. Track-soil interaction produces a reaction force to push the vehicle forward and it imposes a longitudinal slip component [1]. The slip phenomenon has been addressed by many researchers and is currently a key issue in the field of mobile robots working on off-road environments [2]-[6]. Otherwise, an effective kinematic model would allow prediction of the approximate motion of the vehicle in the short term, which is necessary to perform on board real-time computations for autonomous navigation. Ref. [7] proposed a kinematic approach for tracked vehicles by obtaining a geometry analogy with a wheeled differential drive model, by considering the different values of the instantaneous centres of rotation (ICRs) of the tracks. The position of these ICRs depends on the track-soil interactions and some parameters [7], the steering efficiency χ and the normalized eccentricity e, permit to include the effect of the skid-steering robot dynamics.

Other recent and more complex strategies for robots autonomous navigation (i.e. [8], [9], [10]) consider the possibility of constructing intelligent spaces by using a network of distributed sensors. In [8] the data of the mobile robot sensors are compared with the data of distributed external laser sensors for mapping in detail the external environment, in [9] the data for the robot navigation are obtained by using a network of wireless pyroelectric sensors, in [10] a combination between a monocular visual navigation technology and remote monitoring technology is considered.

The use of additional sensors to the simple kinematic information available through the robot encoder data has been recently applied to the kinematic analysis and modelling of skid-steering robots for improving its localization and its odometry. In [11], a covariance intersection filter is

used for fusing the data of a laser scanner with the internal robot sensors (encoders) data for the skid-steering robot position estimation. In [12] an Inertial Unit Based (sensor) is used on skid-steered four wheels robots for estimating, together with the robot internal sensors (encoders), the robot positioning and the kinematic relationship between the wheel slips and locations of the instantaneous rotation centres. In [13] dynamic models for skid-steered vehicles, including resistance terms, have been developed for general motion validating it with some experimental closed loop control tests referred to manoeuvres with small accelerations. In a very recent work [14], a laser scanner sensor has been used on a skid-steering wheeled robot for estimating the relationship between the kinematic parameters χ and the path parameters (curvature radius and robot speed) obtaining an empirical function that permits to improve the motion estimation significantly.

The main contribution of this paper is the analysis of the kinematic parameters χ related to the instantaneous centres of rotation (ICRs) carried out without any additional sensors, but only using the internal robots data and a simple and an innovative geometrical procedure. Moreover, an extensive experimental campaign has been performed by moving the analysed skid-steered robot on surfaces with different characteristics in order to identify the empirical behaviour of the parameters in different slipping conditions. The analysis of other coefficients opportunely introduced, the slipping ratios and the slipping coefficients, estimated by the experiments, permit also to individuate some range of the path parameters (radius of curvature and velocity) where the slipping ratio has a stable value and could easily permit an accurate kinematic planning.

This paper is organized as in the following: in Section II, the kinematic modelling based on the instantaneous centres of rotation of the two tracks on the plane and on the concept of 'equivalent carriageway' is shown. Section III offers a description of the modalities of the experimental tests carried out for the skid steering robot, the Rover 4WD1, aimed to evaluate the 'equivalent carriageway and the slippage coefficient. In Section IV the experimental data with different surfaces are discussed; Section V presents an application of path planning for circumnavigating an obstacle based on the considered procedures, Section VI is devoted to conclusions.

II. KINEMATIC ANALYSIS OF THE SKID-STEERING ROBOTS

In order to clarify the meaning of the following experimental tests, in this section the main equation used in the model of the centres of rotation and on the model of the equivalent carriageway, both based on geometric relationships, are introduced. There is to underline that for control design and reliable simulation of these types of vehicles, the considered kinematic models become an important and valid alternative to the complex dynamic models that may be too costly for real-time robot navigation.

a. Theoretical background on the model based on Instantaneous Centre Radiuses (ICRs) [7]

The local frame of the vehicle is assumed to have its origin on the centre of the area defined by the contact surface of both tracks on the plane, and its Y-axis is aligned with the vehicle forward. The vehicle may be considered as a rigid body following a circular trajectory about ICR_v motion direction. A skid steering vehicle is governed by two control inputs: the linear velocity of its left and right tracks with respect to the robot frame (V_l, V_r).

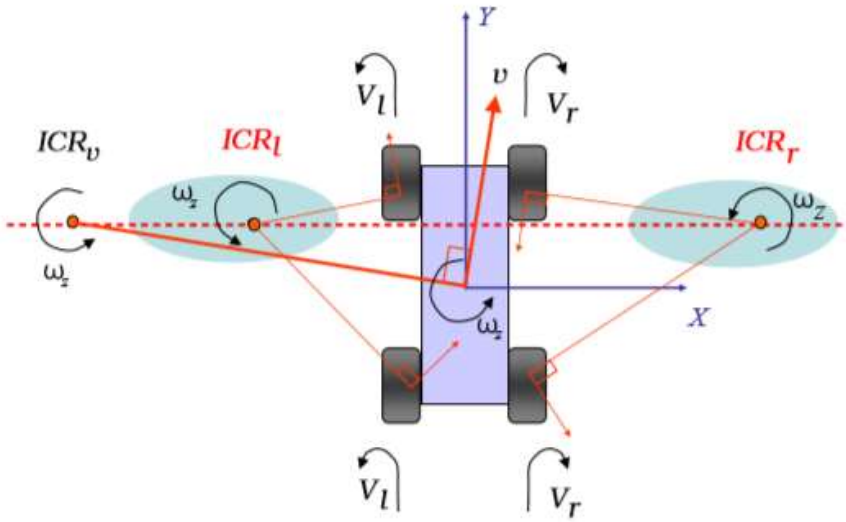

Figure 1. Vehicle model and its ICRs on the plane

Then, direct kinematics on the plane can be stated as follows (1):

$$\begin{pmatrix} v_x \\ v_y \\ \omega_z \end{pmatrix} = f\begin{pmatrix} v_l \\ v_r \end{pmatrix} \tag{1}$$

where $v = (v_x, v_y)$ is the vehicle translation speed and ω_z is the angular speed; inverting the function in Eq.1 it is possible to estimate the velocities of the left and right wheels of the vehicle in order to obtain a corresponding translation and rotation of all the vehicle.

When the robot curves, its ICR on the motion plane may be expressed in local coordinates as $ICR_v = (x_{ICRv}, y_{ICRv})$ (see Fig.1); the left and right ICRs may be defined in a local system as $ICR_l = (x_{ICRl}, y_{ICRl})$ e $ICR_r = (x_{ICRr}, y_{ICRr})$, respectively. It is known [7] that ICR_l and ICR_r lies on the same line parallel to the local X axis (Figure 1) containing ICR_v. Local coordinate for the vehicle and track ICRs can be obtained geometrically as a function of the vehicle's angular and translational velocities as in (2)-(5).

$$x_{ICRv} = -\frac{v_y}{\omega_z} \tag{2}$$

$$x_{ICRl} = -\frac{v_l - v_y}{\omega_z} \tag{3}$$

$$x_{ICRr} = -\frac{v_r - v_y}{\omega_z} \tag{4}$$

$$y_{ICRv} = y_{ICRl} = y_{ICRr} = \frac{v_x}{\omega_z} \tag{5}$$

If the inverse functions are computed from equations (2)–(5), instantaneous translational and rotational speeds, with respect to the local frame, can be obtained. Opportunely combining equations (2)-(5), it is possible to express the kinematic relation in a matrix formulation as in (6) where the matrix A is defined in (7) and it depends only by the ICRs coordinates.

$$\begin{pmatrix} v_x \\ v_y \\ \omega_z \end{pmatrix} = A \cdot \begin{pmatrix} V_l \\ V_r \end{pmatrix} \tag{6}$$

$$A = \frac{1}{x_{ICRr} - x_{ICRl}} \cdot \begin{Bmatrix} -y_{ICRv} & y_{ICRv} \\ x_{ICRv} & x_{ICRl} \\ -1 & 1 \end{Bmatrix} \tag{7}$$

If the ICRs lies symmetrically on the X axis (symmetric model) the A matrix becomes as in (8). In this case, substituting the expression of v_y and ω_z by (6) in (2), it follows (9).

$$A = \frac{1}{2 \cdot x_{ICRr}} \cdot \begin{Bmatrix} 0 & 0 \\ x_{ICR} & x_{ICR} \\ -1 & 1 \end{Bmatrix} \tag{8}$$

$$x_{ICRv} = x_{ICR} \cdot \left(\frac{v_l + v_r}{v_l - v_r} \right) \tag{9}$$

b. The concept of 'equivalent carriageway'

The result expressed in equation (9) is very interesting because the first term represents the radius of the curve trajectory when there is slipping effect and it depends by the internal and external speed and by the position of the rotation centre. It is possible to compare equation (9) with the general expression (10) of the curvature radius R for an ideal robot having wheel track B that does not have any slipping phenomenon while turning on the right ($v_l > v_r$); from the comparison, it is possible to introduce an index χ of the slippage phenomenon, as indicated in Eq. (11).

$$R = \frac{B}{2} \cdot \left(\frac{v_l + v_r}{v_l - v_r} \right) \tag{10}$$

$$\chi = \frac{B}{2 \cdot x_{ICR}} \qquad 0 \le \chi \le 1 \tag{11}$$

The index χ is equal to 1 when there is no slippage and, in this case, the distance between the ICRs of the vehicle is exactly equal to the vehicle wheel track; when χ is smaller than 1, there is slipping and the real radius of curvature R' is defined by $x_{ICR} > B/2 = R$. In other words, the slipping effect increases the curvature radius R' expressed in (12).

$$R' = x_{ICR} \cdot \left(\frac{v_l + v_r}{v_l - v_r} \right) \tag{12}$$

This effect may be considered introducing an 'equivalent carriageway'. The concept of equivalent 'carriageway' may be furtherly clarified considering the carriageway of a 'virtual' mobile robot that describes the same trajectory without slipping maintaining the inner wheel blocked as depicted in Fig. 2.

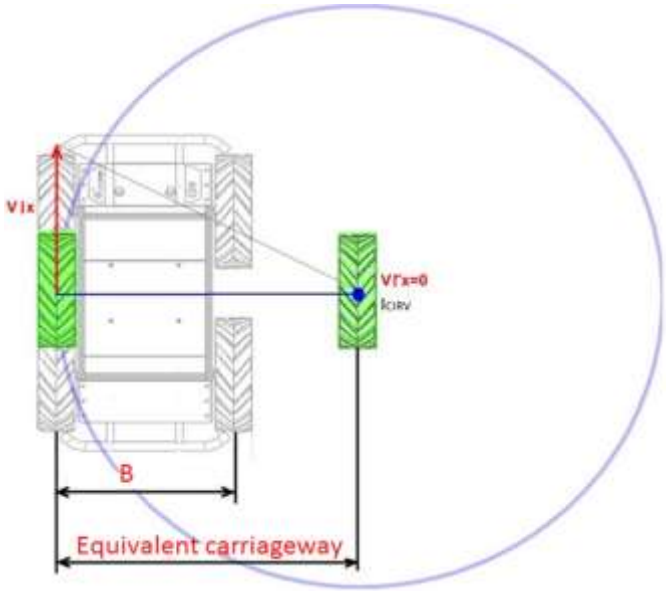

Figure 2. The concept of equivalent carriageway.

c. An alternative method for the slipping evaluation

Another way to keep into account the robot wheels considers an individual percentage slipping of both the wheels. Naming with the subscript 'i' the inner wheel (right wheel in the previous case) and with the subscript 'o' the external wheel (left wheel), with i_i and i_o the slipping coefficients of the inner and external side respectively, it is possible to estimate the effective radius of curvature by (13).

$$R' = \frac{B}{2} \cdot \left(\frac{v_o \cdot (1 - i_o) + v_i \cdot (1 - i_i)}{v_o \cdot (1 - i_o) - v_i \cdot (1 - i_i)} \right) \tag{13}$$

In (13) v_o and v_i are the linear velocities of the external and internal speed, while i_o and i_i are the percentage slipping factors for the external and internal wheel respectively. Defining as K_s the slipping ratio, as defined in (14), equation (13) may be rewritten as in (15).

$$K_S = \left(\frac{1 - i_i}{1 - i_o} \right) \tag{14}$$

$$R' = \frac{B}{2} \cdot \left(\frac{v_o + K_S \cdot v_i}{v_o - K_S \cdot v_i} \right) \tag{15}$$

Equation (15) permits to estimate the radius of curvature R', directly from the knowledge of the velocities of the wheels and from the factor K_s that is characteristic of the field where the mobile robot is moving; in this way, differently from the previous approach (12), the effect of the slippage is clearly highlighted in (15).

The objective of the experimental tests, shown in the following sections, is to estimate the slipping ratio for different operative conditions and for different types of field, in such a way to try to characterize in a general way the kinematic behaviour of the robot.

III. MODALITIES OF THE EXPERIMENTAL TESTS

a. The Rover 4WD1

The approaches described in the previous section are applicable for all types of skid-steering robots. In this paper we'll discuss about the experiments carried out using the Rover 4WD1 (Fig. 3), a very light (the chassis is made by aluminium and lexan) and small robot driven by an appositely designed Matlab interface through which is possible to choose the velocities of the four robot wheels driven by 12 V DC motors through a gear (1:30). A transmitter X-Bee, permits the serial wireless communication between a PC and the robot.

Figure 3. Robot skid-steering Rover 4WD1

All the experimental tests were carried out driving the wheels (diameter 120 mm) of the two sides with different velocities (the wheels of the same side with the same value) and measuring the radius of curvature of the described trajectory. In order to estimate the radius of curvature R also when it is very big and it is not possible for the robot to describe the entire circle a geometrical procedure has been considered. Considering a trajectory (see Fig.4) described by an arch of circle (points A and B) and naming l the length of the segment AB, x its projection on X axis, α the angle corresponding to the arc AB, it is possible to estimate R by (16).

$$R = \left(\frac{l^2}{2 \cdot x} \right) \tag{16}$$

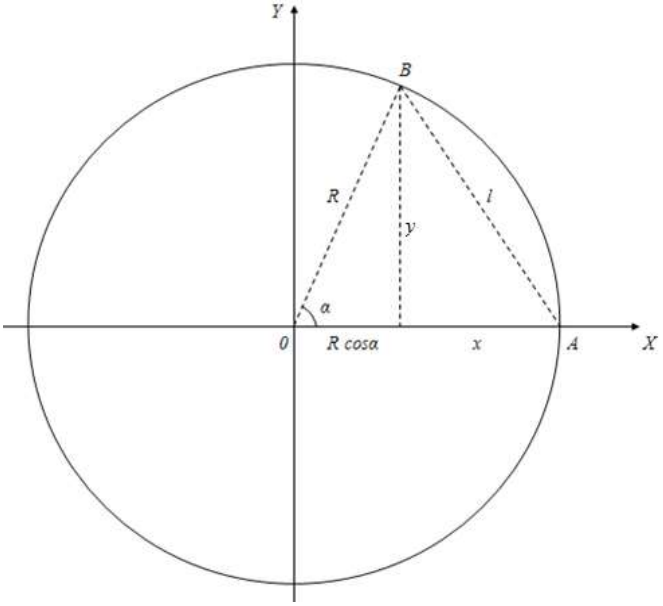

Figure 4. Geometrical evaluation of the radius of curvature R

Eq. (16) may be demonstrated considering the geometrical relations (17) that lead to Eq. (18).

$$\begin{cases} \alpha = \arccos(1 - \frac{x}{R}) \\ sen(\alpha) = \frac{y}{R} \end{cases} \tag{17}$$

$$sen(\alpha) = sen[\arccos(1 - \frac{x}{R})] \tag{18}$$

Using the decomposition of a sine, eq. (18) becomes (19).

$$sen(\alpha) = \sqrt{\frac{x}{R}} \cdot \sqrt{2 - \frac{x}{R}} \tag{19}$$

$$\frac{y}{R} = \sqrt{\frac{x}{R}} \cdot \sqrt{2 - \frac{x}{R}} \tag{20}$$

With simple mathematical passages applied at (20) as expressed in (21), from the last passage of (21), it is possible to demonstrate equation (16).

$$\frac{y^2}{R^2} = \frac{x}{R} \cdot (2 - \frac{x}{R}) \Longrightarrow \quad 2 \cdot x \cdot R = y^2 + x^2 = l^2 \tag{21}$$

IV. EXPERIMENTAL TESTS

As indicated in the previous section, the velocity of the four wheels of the robot are accurately defined through a Matlab code and an Xbee connection; the code attributes an entire value k that may vary from 0 to 127. A preliminary calibration has permitted to verify the correspondence between the values of k and the angular velocities of the wheel. Starting from an angular speed of 0.33 rad/s for k=5 (corresponding to 0.02 m/s of linear velocity of the wheels) and increasing of 10 the values of k, repeating 5 times the tests in each position, the relation between k and the angular speed has resulted perfectly linear as shown in Fig.5. A value of 21.67 rad/s (1.3 m/s) has resulted for a value of k=125, (for values k=0:4, the robot results unable to move).

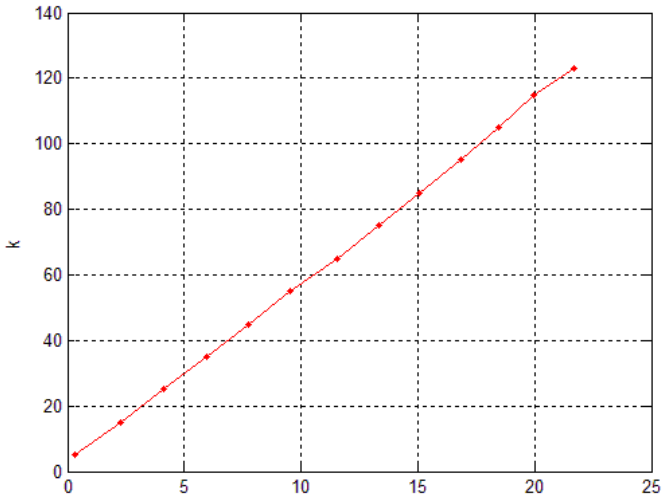

Figure 5. Angular speed in the calibration tests

In order to estimate the equivalent carriage and the slipping ratio with different characteristics of the field, three different surfaces have been considered. The ground floor of the laboratory, named 'indoor' (Fig. 6a), the ground floor outside the laboratory named 'outdoor' (Fig 6.b), smoother than the laboratory surface, and the synthetic grass of a football field named 'football' (Fig. 7). For each surface, 10 sets of experimental tests have been carried out (except from the last surface where only 5 tests were carried out) giving a different angular speed to the wheels of the right side and of the left side of the robot, each of them repeated for three times. Five sets of tests were carried out with a curvature toward the left part and five sets of tests were carried out with a curvature towards the right part. The typologies of set of tests carried out for the different surfaces are summarized in Table I, where the acronyms of the set is indicated (suffix L and R indicate the curvature towards left or right). In Table 1 for each set of tests, the corresponding values of k for the wheels of the right side (named k_r) and the left side (named k_l), the corresponding linear velocities (v_r and v_l for the right and left side respectively) and their absolute value difference (Δv) are indicated.

The sets 1L-5L and 1R-5R are characterized by a constant step of the increase of the difference of the external and internal wheels velocities. Each set indicated in Table I has been repeated for 3 times and, for each repetition, the formula (16) has been applied for determining the radius of curvature; this approach has been performed for all the three types of surfaces except for the 'football surface' where, for simplicity, only the first sets of tests were performed.

Figure 6 a) indoor test

b) outdoor test

c) football pitch test

The repeatability of the experiments has been good, with a very low variation between the measurements of the same set in the same condition (an example of the three measurements of the same test in Fig.8).

Table 1: Definition of the experimental tests sets.

Name	**k_r**	**V_r[mm/s]**	**k_l**	**V_l[mm/s]**	**Δv [mm/s]**
1L	60	632	40	410	222
2L	80	957	40	410	547
3L	80	957	20	191	766
4L	100	1059	20	191	868
5L	120	1249	20	191	1058
1R	40	410	60	632	222
2R	40	410	80	957	547
3R	20	191	80	957	766
4R	20	191	100	1059	868
5R	20	191	120	1249	1058

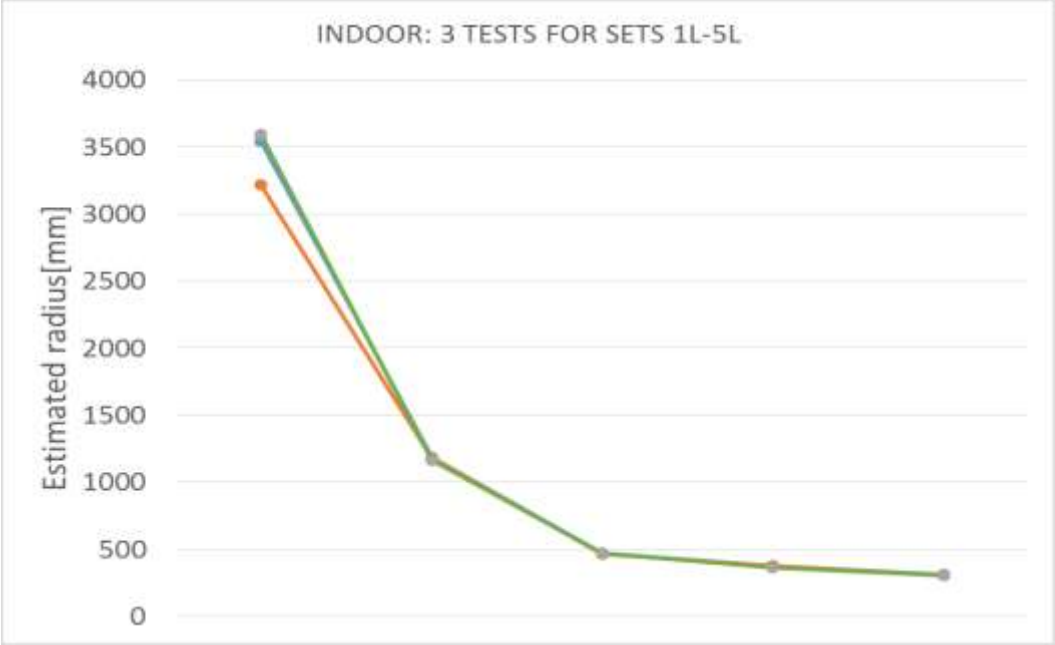

Figure 8. Repeatability test for sets 1L-5L, indoor surface.

The average values of the estimated radius of curvature for all the sets and for all the surfaces are indicated in Table 2. Fig. 8 and Table 2 suggest the following considerations:

- the repeatability of the radius estimation on the same surface is very good and the results are very close; on the contrary the effect of the different surface is very important and the kinematic characteristics of the mobile robot change.
- Considering the same velocity difference, the smaller radius of curvature has been obtained on the indoor surface that means that there is less slipping on that surface respect to the other two considered.
- There is a substantial difference between the sets 1L-5L and the sets 1R-5R; this is probably due to an asymmetry of the robot and its real centre of mass should be moved toward the left part respect to the geometrical centre. This asymmetry could explain the minor slipping of the sets 1L-5L respect 1R-5R in both the surfaces.

A graphical comparison of the differences of the sets 1L-5L for the tree surfaces is shown in Fig.9.

Table 2: Definition of the experimental tests sets.

Name	**Indoor**	**Outdoor**	**Football**
1L	3452	5800	3548
2L	1176	2163	1730
3L	471	687	745
4L	373	496	563
5L	309	387	442
1R	4553	7239	-
2R	1397	2345	-
3R	488	644	-
4R	388	464	-
5R	315	364	-

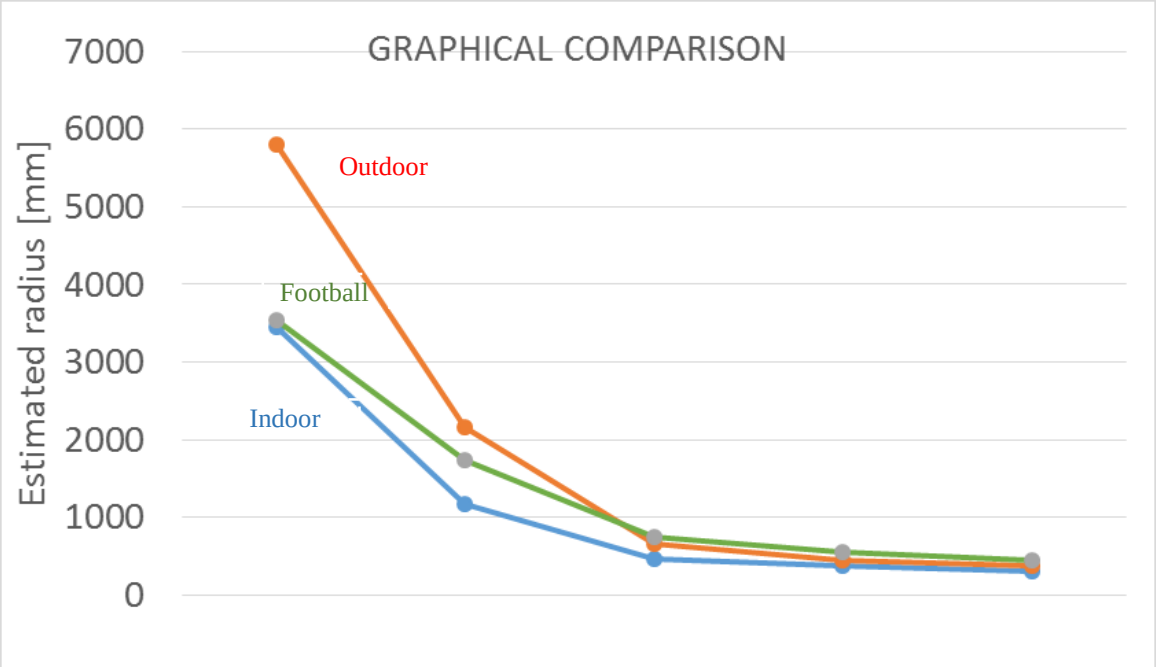

Figure 9. Comparison for sets 1L-5L, data of Table 2.

The estimation of the radius of curvature in the five sets has permitted to fit the experimental data in Fig.9 evaluating for each surface, with a least square method referred to Eq.(12), the equivalent carraiageway x_{ICR} and the slippage index χ (Eq.11) as expressed in Table 3.

Table 3: Estimation of the equivalent carriageway and the slippage index.

Name	**Indoor 1L-5L**	**Indoor 1R-5R**	**Outdoor 1L-5L**	**Outdoor 1R-5R**	**Football**
X_{ICR} [m]	0.247	0.299	0.407	0.467	0.309
χ	0.567	0.468	0.344	0.300	0.453

Once again, from Table 3 it is evident that the best efficiency parameter has been obtained inside the laboratory (Indoor).

Moreover, the estimation of the slipping coefficients may be also carried out evaluating, in percentage, the difference between the encoder data (velocity of each wheel) and the real velocity V_r of the robot measured on the field dividing the distance for the travelling time (22).

$$i = \left(1 - \frac{V_r}{R \cdot \omega}\right) \cdot 100 \tag{22}$$

The estimated slipping coefficients ii for the internal wheel are summarized in Table 4. The suffix 'i' indicates the slipping coefficient for the inner wheel.

Table 4: Slipping coefficients i_i [%]

Name	Indoor	Outdoor	Football
1L	10.4	11.5	2
2L	24.4	23.9	1.7
3L	85	88	48.5
4L	78.7	100	80
5L	71.3	88.9	93.3
1R	16.6	13.6	-
2R	22.7	30.4	-
3R	67.5	75.8	-
4R	91	90	-
5R	79.5	84.1	-

From the data in Table 4, it is evident in all the cases that the percentage slipping increases with the increase of the velocity difference; the dragging effect of the quicker wheel respect to the lower one, becomes always more important with the increasing of the velocity difference.

Comparing the different surfaces, the slipping on the football pitch seem to be the lowest; this is probably due to the different typology of the grass material that may apply forces of adherence more consistent.

Finally, the slipping ratio K_s has been estimated in all the sets using equation (14) as summarized in Table 5. Analysing the values of K_s in Table 5 it is evident that the slipping ratio increases with the increasing of the velocity difference and then it stabilizes itself to a constant value depending only from the surface: the value 2.5 for indoor, 3 for outdoor, 3.5 for football pitch. Considering these values, equation (15) may permit to calculate the radius of curvature for the considered surfaces. This last result is very important because it defines, for this particular type of skid-steering robot, a kinematic parameter that seems to be almost constant for a certain range of the path parameters (tests 3L-5L, tests 3R-5R) and with a small variation depending from the

different surfaces. The considerations shown in this section may be considered the starting point for a possible kinematic reconstruction based only on internals sensors (motor encoders) that considers the slipping effects.

Table 5: Slipping ratio K_s

Name	**Indoor**	**Outdoor**	**Football**
1L	1.42	1.47	1.42
2L	1.83	2.07	1.98
3L	2.71	3.21	3.41
4L	2.54	2.97	3.29
5L	2.45	2.89	3.44
1R	1.45	1.48	-
2R	1.91	2.07	-
3R	2.75	3.21	-
4R	2.6	2.97	-
5R	2.54	2.89	-

V. PATH PLANNING FOR THE CIRCUMANIVAGATION OF AN OBSTACLE

A simple application of the results shown in the previous section has been realized considering the path planning for circumnavigating the obstacle shown in Fig. 10 a (70 cm x 125 cm) on the laboratory surface (Indoor) for the Rover 4WD1. The ideal path (indicated in Fig. 10 b, starting point the point A) is composed by four consecutive stretches: two rectilinear sectors (from the point A to B and from the point C to D in Fig. 10 b) and two curvilinear sectors (from B to C and from D to A). The total length of the circuit is 815.48 cm, each rectilinear path is 125 cm, the radius of curvature of the curvilinear sectors is 90 cm and the length of each arch BC and DA is about 282.74 cm. It is possible to calculate (directly from the calibration curve of Fig.5) the values of k in the rectilinear sectors after choosing a linear velocity for the rectilinear sectors. In the other sectors, by knowing the slipping ratios K_s (from Table 5), the geometry of the robot and

the angular robot speed ω_z, it is possible, from (6) and (15), to calculate the values of the driving parameter k for the left side and the right side of the robot.

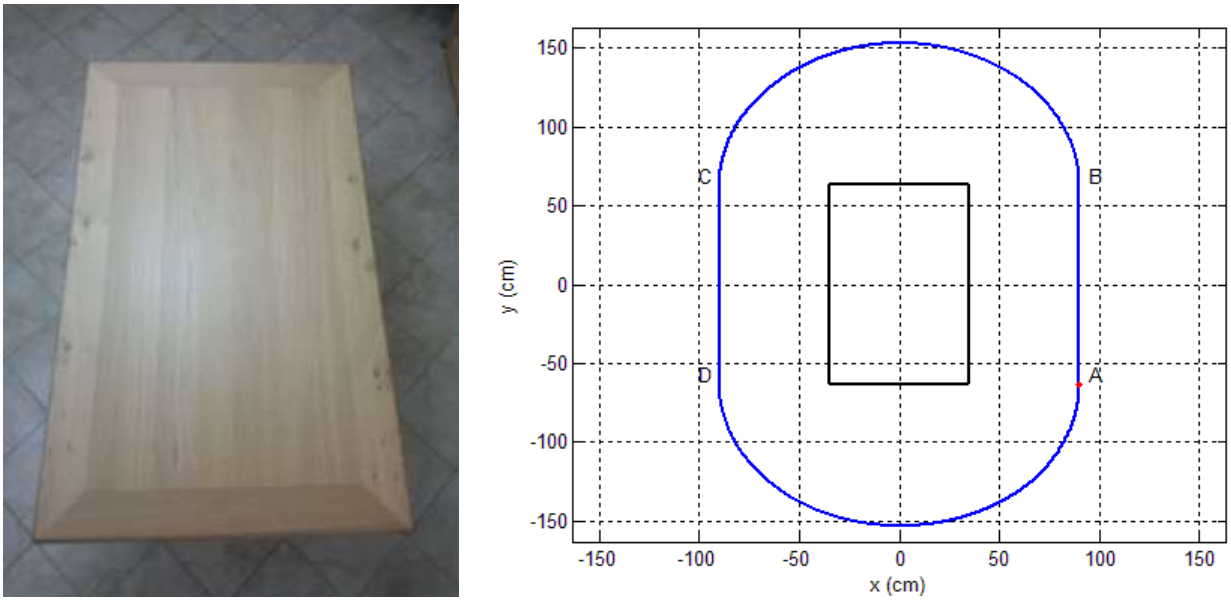

Figure 10. a) obstacle to circumnavigate b) scheme of the path planning (starting point in A)

Five experiments were carried out considering a driving value of k=60 in the rectilinear part (corresponding to an angular speed of 10.5 rad/s, linear velocity 1.26 m/s) and an angular speed of 0.5 rad/s for the curvilinear part that correspond to a value of k =65 (outer wheels) and k=26 (inner wheels).

The results of the five tests are depicted in Fig.11 a) with black points and zoomed in Fig. 11b) where it is clear that the final position is very close to the desired one (red point), with a final error, for all the tests, of a few centimetres after a circuit or more than eight meters.

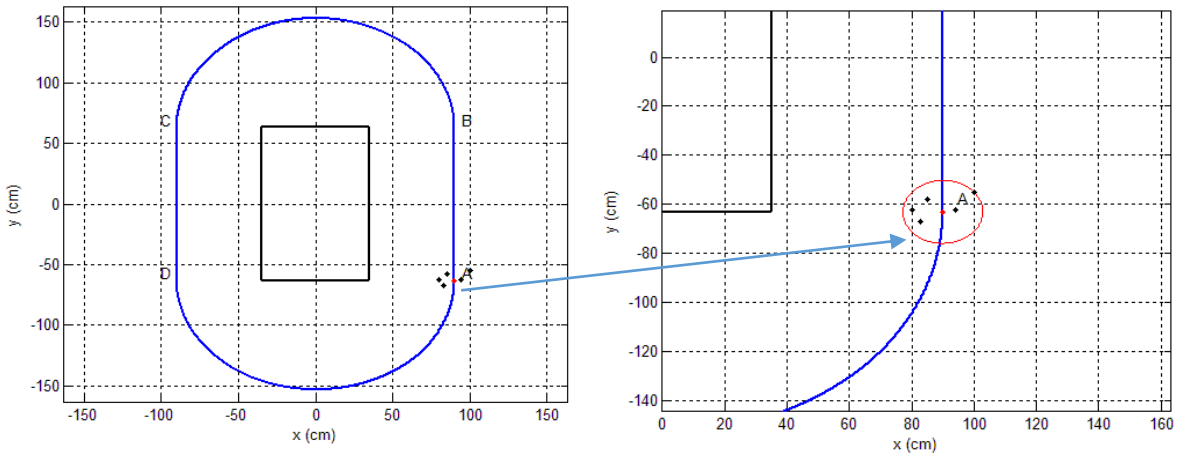

Figure 11. a) Results of the path planning tests b) Zoom of the results

VI. CONCLUSIONS

In this work, the problem of the kinematic modelling of skid-steered robot heavily subjected to slipping effect has been analysed. An innovative procedure, that uses only the internal sensor of the robot, has been presented and applied for evaluating the relation between the robot path parameters and some kinematic coefficients that include the effect of the vehicle dynamic, which is very important for this type of mobile robots. An extensive experimental campaign has been carried out considering different surfaces in order to obtain an empirical evaluation of the kinematic parameters. The experiments clearly show that the typology of slipping depends on the characteristics of the surface; anyway, the possibility of creating a noted relation between the surface type and the kinematic behaviour through the parameters indicated in this paper, may become a successfully achieved target of the next years.

Moreover, an interesting result obtained is that, in a limited range of robot path parameters, one coefficient (the slipping ratio K_s), has a limited variation and it may be used for reconstructing the kinematic trajectories including the slipping effect and also for realising a path planning in a very simple way and without using additional sensors.

Actual researches are focused on the possibility of generalizing the proposed approach to different types of vehicles in order to obtain a general model for driving accurately this typology of robots with respects to different types of surfaces and to the geometrical characteristics of the considered vehicles.

REFERENCES

[1] Wong, J. Y.: 'Theory of ground vehicles, Third Edition'. J.Wiley & sons, Inc.

[2] Al-Milli, S., Severinatne, L. D., Althofer, K.: 'Track-terrain modelling and traversability prediction for tracked vehicles on soft terrain' Journal of Terramechanics, 2010, 47, pp. 151–160.

[3] Gonzales, R., Rodriguez, F., Guzman, J.L., Berenguel, M.: 'Localization and control of tracked mobile robots under slip cnditions' Proc. Of the 2009 IEEE International Conference on Mechatronics, Spain, 2009, pp. 1-6.

[4] Dar, T.M., Longoria, R.G.: 'Slip estimation for small-scale robotic tracked vehicle', Proc. Of 2010 American Control Conference, USA, 2010, pp. 6816-6821.

[5] Burke, M.: 'Path-following control of a velocity constrained tracked vehicle incorporating adaptive slip estimation' Proc. Of 2012 IEEE International Conference on Robotics and Automation, USA, 2012, pp.97-102.

[6] Mandow, A., Martinez, J.L. Morales, J., Blanco, J.L., Garcia-Cerezo, A., Gonzalez, J.: 'Experimental kinematics for wheeled ster.steering robots' Proc. of IROS, USA, 2007, pp.1222-1227.

[7] Martinez, J. L., Mandow, A., Morales, J., Pedraza, S., Garcia-Cerezo, A.: 'Approximating kinematics for tracked mobile robots', The International Journal of Robotics Research, 2005, 24 (10), pp. 867-878.

[8] Hashikawa, F., Morioka K.,: 'An assistance system for building intelligent spaces based on mapsharing among a mobile robot and distributes sensors', International Journal of Smart Sensing and Intelligent Systems, 2015, 8 (1), pp. 1-25.

[9] Shen, B., Wang, G.:' Distributed target localization and tracking with wireless pyroelectric sensor networks' International Journal of Smart Sensing and Intelligent Systems, 2013, 6 (4), pp. 1400-1418.

[10] Wang, Y., Yang, F., Wang, T. Liu, Q., Xiudong, X.' Research on visual navigation and remote monitoring technology of agricultural robot' International Journal of Smart Sensing and Intelligent Systems, 2013, 6 (2), pp. 466-481.

[11] Anousaki, G., Kyriakopoulos, K. 'Simultaneous localization and map building of skid-steered robots', IEEE Robotics and Automation Magazine, 2007, 14, pp. 79-89.

[12] Yi, J., Wang, H.P., Zhang, J., Song, D. 'Kinematic modelling and analysis of skid-steered mobile robots with applications to low-cost inertial-measurement-unit-based motion estimation', IEEE Transactions on Robotics, 2009, 25 (5), pp. 1087-1097.

[13] Yu, W., Chuy, O., Collins, E.G., Hollins, P. 'Analysis and experimental verification for dynamic modelling of a skid-steered wheeled vehicle', IEEE Transactions on Robotics, 2010, 26 (2), pp. 340-353.

[14] Wang, T., Yao, W., Liang, J. Han, C., Chen, J., Zhao, Q. 'Analysis and experimental kinematics of a skid-steering wheeled robot based on a laser scanner sensor' Sensors, 2015, 15, pp. 9681-9702.